Acta Pharmaceutica Sinica B 2024;14(4):1592−1604

Chinese Pharmaceutical Association
Institute of Materia Medica, Chinese Academy of Medical Sciences

Acta Pharmaceutica Sinica B

www.elsevier.com/locate/apsb
www.sciencedirect.com

TOOLS

Construction and characterization of a humanized *SLCO1B1* rat model with its application in evaluating the uptake of different statins

Yuanjin Zhang, Junze Huang, Shengbo Huang, Jie Liu, Luyao Deng, Chenmeizi Liang, Yuanqing Guo*, Bingyi Yao*, Xin Wang*

Changning Maternity and Infant Health Hospital and School of Life Sciences, Shanghai Key Laboratory of Regulatory Biology, East China Normal University, Shanghai 200241, China

Received 21 September 2023; received in revised form 28 November 2023; accepted 6 December 2023

KEY WORDS

CRISPR/Cas9;
Drug transport;
Drug disposition;
Gene editing;
Humanized rat model;
OATP1B1;
SLCO1B1;
Statins

Abstract Organic anion-transporting polypeptides 1B1 (OATP1B1) plays a crucial role in the transport of statins. However, there are too few animal models related to OATP1B1, especially humanized animal models. In this study, the human *SLCO1B1* cDNA was inserted into the second exon of the rat *Slco1b2* gene using CRISPR/Cas9 technology. Pharmacokinetic characteristics of statins were conducted in wild-type (WT), humanized OATP1B1 (*h*OATP1B1), and OATP1B2 knockout (OATP1B2 KO) rats, respectively. The results showed that human OATP1B1 was successfully expressed in rat liver and exhibited transport function. Furthermore, the pharmacokinetic results revealed that OATP1B1 exhibited varying uptake levels of pivastatin, rosuvastatin, and fluvastatin, leading to different levels of exposure within the body. These results were consistent with those obtained from *in vitro* experiments using overexpressed cell lines. In conclusion, we established a novel humanized *SLCO1B1* transgenic rat model to assess the role of human OATP1B1 in the uptake of different statins. The different uptake mediated by OATP1B1 may be an important reason for the different efficacy of statins. The *h*OATP1B1 rat is a promising model for improving the prediction of human drug transport.

*Corresponding authors.
E-mail addresses: xwang@bio.ecnu.edu.cn (Xin Wang), 13816852233@163.com (Bingyi Yao), gyqrose@126.com (Yuanqing Guo).

Peer review under the responsibility of Chinese Pharmaceutical Association and Institute of Materia Medica, Chinese Academy of Medical Sciences.

https://doi.org/10.1016/j.apsb.2023.12.019

1. Introduction

Statins, also known as the HMG-CoA reductase inhibitors, are nearly the most prescribed drugs in the world for the treatment of myocardial infarction, ischemic stroke, and other complications of atherosclerotic diseases[1,2]. Statins reduce plasma low-density lipoprotein cholesterol (LDL-C) levels by inhibiting HMG-CoA reductase, which plays a key role in liver cholesterol production, thereby reducing the incidence of cardiovascular disease[3,4]. Studies have shown that long-term administration of statins is effective for both primary and secondary prevention of cardiovascular events[5–7]. Even more exciting, recent studies have shown that statins have a substantial preventive effect against liver disease[8] and that statins may improve endothelial function by inhibiting epigenetic-driven endothelial-to-mesenchymal transition (EndMT)[9].

Currently, there are seven statins (rosuvastatin, atorvastatin, simvastatin, pitavastatin, lovastatin, pravastatin, and fluvastatin) that are readily available and have been proven to be well tolerated[5]. Although statins are generally considered safe, their systemic exposure may be influenced by drug−drug interactions (DDI), which may increase the risk of statin-associated muscle symptoms (SAMS)[10,11]. These interactions are predominantly facilitated by metabolic enzymes, primarily cytochrome P450 (CYP) isoenzymes, and membrane-bound transporters, including P-glycoprotein (P-gp) and organic anion-transporting polypeptides (OATPs)[11,12]. However, the metabolism and transport of statins is far from well understood. For example, the contribution of different OATPs in mediating statin transport remains unclear.

OATPs are recognized as important transmembrane proteins that mediate the cellular uptake of a wide variety of substrates and have a great impact on the systemic pharmacokinetics of many drugs[13,14]. The seven marketed statins are well recognized as substrates for OATP1B1, OATP1B3, and OATP2B1[15,16]. OATP1B1 (encoded by the *SLCO1B1* gene) is one of the best-characterized OATPs and is highly expressed mainly on the basolateral (sinusoidal) membrane of human hepatocytes[17,18]. Studies have shown that OATP1B1 is a genetic polymorphism transporter, and function-related single nucleotide polymorphisms (SNPs) have been identified. Numerous studies have confirmed the importance of OATP1B1 in the clinical efficacy and adverse reactions of statins, with a focus on *SLCO1B1* SNPs[18–20]. In addition, due to the presence of SAMS and SNPs, more and more research has focused on statin-related DDI mediated by OATP1B1[10–12]. Therefore, it is critical to recognize the contribution of OATP1B1 to statin uptake to ensure their safe administration. Of course, it is also important to identify specific inhibitors or inducers of OATP1B1.

A large amount of gene replication and differentiation occurs in the rodent OATP1 family compared to humans, which complicates direct comparisons between studies of the two species[21]. There are two subtypes of OATP1B transporters in humans (OATP1B1 and OATP1B3) and only one in rodents (OATP1B2). Because species differ significantly in DNA sequence, protein expression, and substrate specificity, extrapolation of results obtained from traditional preclinical animal models to humans is limited[22,23]. Therefore, it is not reasonable to study the transport properties of OATP1B1 and its contribution to the uptake of statins in rodents, due to species differences in the OATP1 family. However, the emergence of genomically humanized animals could overcome species differences to a certain extent, which is conducive to the construction of human disease models as well as drug metabolism and transport research[24,25].

In this study, we successfully constructed and characterized a humanized OATP1B1 rat model using CRISPR/Cas9 technology. In the genomically humanized rats, the expression of the human gene (*SLCO1B1*) and protein (OATP1B1) accurately mimicked the human situation. More importantly, we evaluated the contribution of OATP1B1 to statin uptake in rats for the first time. Therefore, the humanized rat model could be used to predict human drug transport, which will certainly facilitate drug development. Furthermore, our findings will also provide valuable guidance on the clinical safety of statins.

2. Materials and methods

2.1. Chemicals and reagents

The DNA polymerase (2 × Phanta Max Master Mix), T7 Endonuclease I (T7E I), and DNA extraction mini kit were purchased from Vazyme (Nanjing, China). DNA extraction reagent (phenol: chloroform: isoamyl alcohol = 25:24:1, *v*/*v*/*v*) was gained from Solarbio (Beijing, China). The BCA protein quantification kit was acquired from Thermo Scientific (Waltham, MA, USA). *pEASY*-Blunt Cloning Kit was purchased from TransGen Biotech (Beijing, China). The MagZol Reagent and Hipure Plasmid EF Maxi Kit were bought from Magen (Guangzhou, China). T4 ligase and restriction endonucleases (NotI and NheI) were purchased from Beyotime Biotechnology (Shanghai, China). The PEI was obtained from Polysciences (Warrington, PA, USA). The OATP1B1 rabbit primary antibody (A15783) was bought from ABclonal Technology (Wuhan, China), and the anti-GAPDH antibody (ab8245) was purchased from Abcam (Cambridge, UK). The fluorescence-conjugated secondary antibody to rabbit and mouse IgG was gained from Cell Signaling Technology (Boston, MA, USA). The cDNA synthesis SuperMix, qPCR SYBR green master mix, and DNA marker were acquired from Yeasen Biotechnology (Shanghai, China). Statins (including pitavastatin, rosuvastatin, and fluvastatin) were purchased from Meilunbio (Dalian, China). Acetonitrile, formic acid, and ammonium formate (all HPLC grade) were gained from Fisher Chemicals (Leicester, UK).

2.2. Animals and ethical issues

Wild-type (WT) Sprague−Dawley rats were supplied by National Rodent Laboratory Animal Resources (Shanghai, China). *Slco1b2* knockout rats (*Slco1b2*$^{-/-}$, KO) were generated by CRISPR/Cas9 in our previous study[26]. All rats used in this study were kept in a specific-pathogen-free (SPF) barrier with free access to eat and drink. All animal experiments complied with relevant ethical regulations, and the animal procedures were performed under the approval of the Ethics Committee on Animal Experimentation of East China Normal University (Ref. No. R20210211).

2.3. Construction of the humanized OATP1B1 rat

2.3.1. Target-site selection and single guide RNA (sgRNA) synthesis

The *Slco1b2* gene sequence of *Rattus norvegicus* (Norway rat) was obtained from the National Center for Biotechnology Information (https://www.ncbi.nlm.nih.gov/). Two splicing site sequences targeting the second exon (right next to the start codon) of the *Slco1b2* gene were selected, which includes a protospacer adjacent motif (PAM) site in the 3′ end. The 23 bp target sequence

is 5′-CTTTCCTTGACTGCTGAGTGTGG-3′ and 5′-AAGGTTC TGCGATGGATTCAAGG-3′. The PAM site is TGG and AGG, respectively. The two sgRNA sequences were synthesized by GenScript (Nanjing, China).

2.3.2. Donor template generation

The homologous arm sequence was amplified with DNA polymerase (2 × Phanta Max Master Mix) and primers, which included the left homologous arm sequence (HA-L, 975 bp), right homology arm sequence (HA-R, 689 bp) and the splicing site sequence. The amplification conditions and procedures were performed according to the instructions. After purification with a DNA extraction kit, the PCR product of the homologous arm sequence was ligated to the blunt cloning vector with a *pEASY*-Blunt Cloning Kit. Then, after transfection, cloning, sequencing, and culturing, the newly formed plasmid was extracted from the bacteria with the Hipure Plasmid EF Maxi Kit. The pENTER plasmid containing human *SLCO1B1* CDS sequence and C terminal flag and his flag were supplied from WZ Biosciences Inc. (Jinan, China). As shown in Fig. 1, to obtain linear PCR products containing the target sequence, pEASY and pENTER plasmids gained above were used as templates, and two pairs of primers were designed ingeniously (Supporting Information Table S1). Vectors and insertion sequences with homologous ends (overlap) were purified, and both fragments were added to the Gibson assembly master mix. Finally, the plasmid containing the donor template was obtained and then linearized by PCR amplification.

2.3.3. Embryo microinjection

The method of acquiring pseudopregnant rats and embryos was the same as we reported earlier[26]. The cas9 mRNA (10 ng/μL), sgRNA (10 ng/μL), and 100 ng/μL of donor template were co-injected into the embryos by microinjection technology. Then, after proper culturing, the viable embryos were transferred to the fallopian tubes of the pseudo-pregnant rats for normal breeding.

2.4. Genotype identification

The newborn rats after microinjection were defined as the F0 generation. The genomic DNA was extracted from the toes of newborn rats with phenol/chloroform reagent. After amplification with DNA polymerase and primers (Table S1), the PCR products (2863 bp) were electrophoresed on the 1.5% agarose gel. PCR products of the F0 generation with the correct band position were sent to GENEWIZ (Suzhou, China) for Sanger sequencing to ensure accurate sequences. The identified F0 offspring were caged with WT rats to obtain heterozygous F1 generation. Then after electrophoresing and sequencing, the healthy adult male and female F1 rats were selected and caged to breed homozygous F2 generation. The F2 rats also need to be genotyped before proceeding to the further experiment.

2.5. Off-target site detection

The two splicing site sequences were entered into the target analysis website (https://benchling.com) to gain off-target information. Several potential sites (score >1.5, Supporting Information Table S2) were selected for off-target detection as described before[26]. The primer pairs used for off-target effect detection are listed in Table S1.

2.6. Detection of OATP1B1 expression

2.6.1. Real-time quantitative PCR

Total RNA was isolated from the livers of WT and *h*OATP1B1 rats using the MagZol Reagent according to the experiment protocols. Two micrograms of total RNA were quantitatively reverse-transcribed using the cDNA synthesis SuperMix kit. Then the cDNA was performed with qPCR SYBR green master mix kit, and the relative mRNA content of *Slco1b2* and *SLCO1B1* was analyzed by real-time quantitative PCR using Quant Studio 3 Real-Time PCR System (ThermoFisher Scientific). Primer information is listed in Table S1. The β-actin was used as the internal control.

2.6.2. Western blotting

Tissue from snap-frozen liver was homogenized in RIPA working solution. Standard Western blotting analysis was performed in 10% SDS-PAGE gels (40 μg per well) and transferred to the nitrocellulose membrane. Membranes were blocked for 2 h with 5% BSA, followed by incubating with primary antibodies overnight at 4 °C. Rabbit anti-OATP1B1 (1:1000) and rabbit anti-GAPDH (1:20,000) were used as the primary antibody. Secondary antibody incubations were done at room temperature for 1 h using goat anti-rabbit antibody (1:10,000) and then scanned by Odyssey imager system (LI-COR, MA, USA).

2.6.3. Immunohistochemistry

The liver tissue was fixed with a 4% paraformaldehyde (PFA) solution. The following steps were entrusted to Servicebio Co., Ltd. (Wuhan, China). The primary antibody, rabbit anti-OATP1B1 (1:500), was supplied by ourselves.

2.7. Compensatory effects evaluation

The mRNA levels of major absorptive transporters, efflux transporters, and CYP enzymes were detected to evaluate the compensatory effects of *SLCO1B1* knockin. The detection method and primers used were consistent with our previous reports[26,27].

2.8. Physiological condition detection

2.8.1. Hematoxylin & eosin staining

Entrusted to Servicebio Co., Ltd. (Wuhan, China), the paraffin slices were prepared and stained with hematoxylin and eosin (H&E) according to standard procedures.

2.8.2. Physiological indicators of blood lipids and liver function

Physiological indexes of serum were detected by biochemical kits, which were purchased from Nanjing Jiancheng Bioengineering Institute (Nanjing, China). The absorbance was measured by SuPerMax 3000FA (Flash Spectrum Biotechnology, Shanghai, China). Blood lipid indexes include triglyceride (TG), total cholesterol (TC), high-density lipoprotein cholesterol (HDL-C), and low-density lipoprotein cholesterol (LDL-C). Liver function indicators include total bilirubin (TBIL), direct bilirubin (DBIL), total bile acid (TBA), total protein (TP), albumin (ALB), alkaline phosphatase (ALP), aspartate aminotransferase (AST), and alanine aminotransferase (ALT).

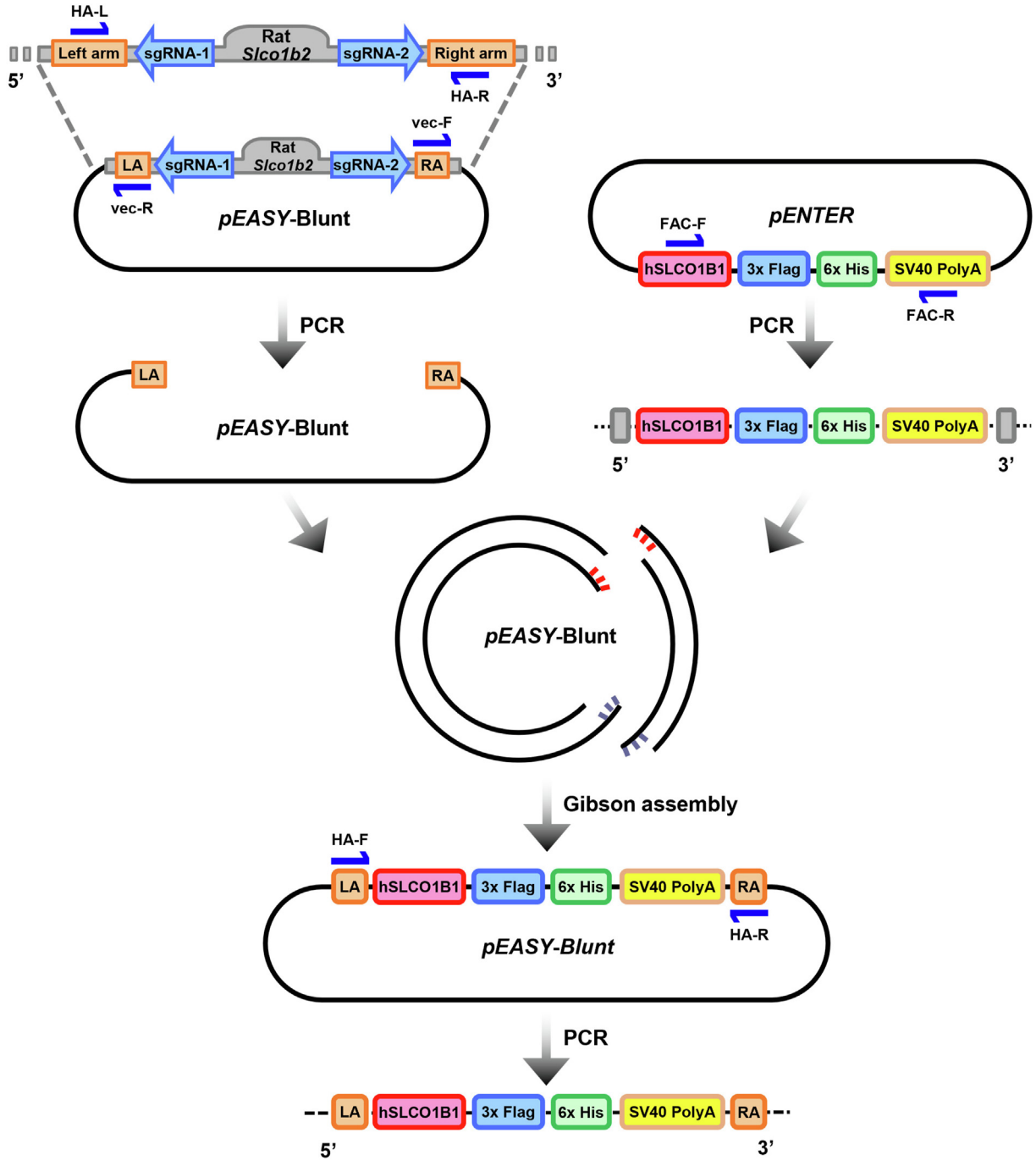

Figure 1 Construction of *hSLCO1B1* donor template. The homologous arm sequence including HA-L, HA-R, and the splicing site sequence was ligated to the *pEASY*-Blunt vector. The pENTER plasmid containing human *SLCO1B1* CDS sequence and C terminal flag and his flag was supplied from WZ Biosciences Inc. Then pEASY and pENTER plasmids were used as templates and two pairs of primers (vec-F/R and FAC-F/R) were designed ingeniously. Vectors and insertions sequences with homologous ends (overlap) were purified, and both fragments were added to the Gibson assembly master mix. Finally, the plasmid containing the donor template was obtained and then linearized by PCR amplification.

2.9. Quantification of bile acids

The content of bile acids in the serum was monitored to assess the role of OATP1B1 in endogenous substance transport. The 1290 HPLC (Agilent Technologies) coupled to a quadrupole time-of-flight (AB Sciex TripleTOF 6600) was used for metabolomics studies in Applied Protein Technology Co., Ltd. (Shanghai, China)[28].

2.10. Pharmacokinetic studies of statins

To evaluate the function of OATP1B1, we explored the pharmacokinetic behavior of pitavastatin, rosuvastatin, and fluvastatin in WT, *h*OATP1B1, and OATP1B2 KO rats, respectively. After fasting for 12 h, 5 mg/kg (1 mg/mL) of pitavastatin, 10 mg/kg (2 mg/mL) of rosuvastatin, and 5 mg/kg (1 mg/mL) of fluvastatin were administrated intragastrically. Blood samples were

collected through the tail vein to obtain plasma after administration at 0.17, 0.5, 1, 1.5, 2, 3, 4, 6, 8, 10 h for pitavastatin, 0.25, 0.5, 1, 1.5, 2, 3, 5 h for rosuvastatin, and 0.083, 0.25, 0.5, 0.75, 1, 1.5, 2, 4, 6, 8, 12, 24 h for fluvastatin.

2.11. *Quantification of statins by LC−MS/MS*

The concentrations of pitavastatin, rosuvastatin, and fluvastatin in plasma were quantified with an Agilent 1290 HPLC system, coupled with a 6470 triple-quadrupole mass spectrometer (Agilent Technologies, USA). The detection condition of pitavastatin was as same as previously reported[26]. Unlike pitavastatin, rosuvastatin and fluvastatin plasma samples were treated with protein precipitation. Dexamethasone (100 ng/mL) was used as the internal standard. Specific measurement conditions are shown in Supporting Information Table S3.

2.12. *Cell culture*

Referring to the previous method[29], we constructed and verified OATP1B1 and OATP1B2 overexpression cell models. Then the uptake of pitavastatin, rosuvastatin, and fluvastatin was detected. The empty pCDH (pCDH-EF1-MCS-T2A-copGFP) vector was used as a blank control. After drug treatment (10 μmol/L), cell lysis, and sample processing, the concentration of statins was quantified by LC−MS/MS.

2.13. *Molecular docking analysis*

Computational modeling methods were used to further elucidate the binding affinity of OATP1B1 with pitavastatin, rosuvastatin, and fluvastatin. The protein information of OATP1B1 was gained from UniProt (UniProtKB: A0A024RAU7). Small molecules may bind to the loop region (located on the outside of the transmembrane structure) and transmembrane helices during transport. AutoDock Vina (version 1.2.0) was applied for molecular docking analysis[30].

2.14. *Statistical analysis*

All statistical analysis and all graphs presented in this paper were performed using GraphPad Prism (version 8.0.1, GraphPad Software, San Diego, CA, USA). All data are shown as mean ± standard deviation (SD). A two-tailed Student *t*-test was used when statistical analysis between two groups was performed and the one-way analysis of variance (ANOVA) statistical method was used for multiple comparisons. Based on non-compartmental analysis, pharmacokinetic parameters of pitavastatin, rosuvastatin, and fluvastatin were calculated by WinNonlin software version 5.2.1 (Pharsight Corporation, Mountain View, USA). The pharmacokinetic parameters include elimination half-life ($t_{1/2}$), maximum concentration (C_{max}), time to reach C_{max} (T_{max}), area under the concentration−time curve (AUC), apparent volume of distribution/bioavailability (V_d/F), clearance/bioavailability (CL/F), and mean residence time (MRT). The P-value less than 0.05 was considered significant ($^{*}P < 0.05$, $P < 0.01$, and $P < 0.001$ or $^{\#}P < 0.05$, $^{\#\#}P < 0.01$, and $^{\#\#\#}P < 0.001$).

3. Results

3.1. *Generation of humanized OATP1B1 rats by CRISPR/Cas9*

The donor template is a key component in the construction of humanized OATP1B1 rats. As shown in Fig. 1, the linearized PCR product of the donor template was successfully generated, and the correctness of the base sequence was ensured by Sanger sequencing. The schematic diagram of the target design is presented in Fig. 2A. After co-microinjection with sgRNA and Cas9 mRNA, fifteen F0 generation rats were born. Results of agarose gel electrophoresis indicated that the donor template was successfully inserted at the target site of F0-12# and 14# rats (Fig. 2B). Further sequencing revealed that only F0-12# rat had the correct insertion sequence. The F1 generation rats (heterozygotes) were obtained from the cage of F0 generation and WT rats. Then healthy male and female F1 generation rats with correct sequence were selected to breed homozygous F2 generation rats (Fig. 2C). To assess the off-target effects of the two sgRNAs, seven potential sites were detected. The results showed that no off-target effect was observed (Supporting Information Fig. S1A and S1B). The expression of OATP1B1 at the mRNA level was detected in WT and *h*OATP1B1 rats. The results showed that *Slco1b2* and *SLCO1B1* were specially expressed in the liver of WT and *h*OATP1B1 rats, respectively (Fig. 2D and E). To evaluate the effects of *SLCO1B1* knockin on the transporter and metabolic enzyme-related genes, the mRNA levels of major uptake transporters, efflux transporters, and CYP enzymes were detected. As presented in Supporting Information Fig. S2A−S2C, no statistically significant changes were found between WT and *h*OATP1B1 rats. Western blot results revealed that OATP1B1 was successfully expressed in the liver of *h*OATP1B1 rats but not in WT rats (Fig. 2F). The immunohistochemical results confirmed that OATP1B1 was highly expressed on the sinusoidal membrane of the *h*OATP1B1 rat liver (shown in brown, Fig. 2G).

3.2. *Evaluation of the physiological status of humanized OATP1B1 rats*

Healthy physiological status is an important prerequisite for OATP1B1 to exert its transport function. As shown in Fig. 3A−D, compared with WT, there were no abnormalities in the blood lipids of *h*OATP1B1 rats. According to the results of H&E staining (Fig. 3E), the hepatocyte morphology of *h*OATP1B1 rats did not change significantly. Previous reports have found that the decrease or loss of OATP1B1 function significantly increases blood levels of bilirubin and bile acids[20,26]. Therefore, the determination of these two endogenous substances in serum can reflect whether OATP1B1 performed the transport function. The results showed that there was no significant difference in serum TBIL and DBIL contents of WT rats and *h*OATP1B1 rats, and both were significantly lower than those in OATP1B2 KO rats (Fig. 3L and M). There was a three-fold increase in serum TBA in *h*OATP1B1 rats compared with WT rats and a 78% decrease in serum TBA compared with OATP1B2 KO rats (Fig. 3N). These results suggest that OATP1B1 performed the transport function. The reason for the elevated content of TBA in *h*OATP1B1 rats is that OATP1B2 has a stronger transport capacity for TBA than OATP1B1 (no OATP1B3 in *h*OATP1B1 rats). In addition, untargeted metabolomics methods were used to obtain the metabolic profiles of serum samples. The results also showed that the insertion of the *SLCO1B1* gene only slightly affected the bile acid-related pathway, and OATP1B1 could mediate bile acid transport (Fig. 4A and B). Furthermore, the contents of TP, ALB, AST, ALT, AST/ALT, and ALP were measured, and no significance was found between WT and *h*OATP1B1 rats (Fig. 3F−K).

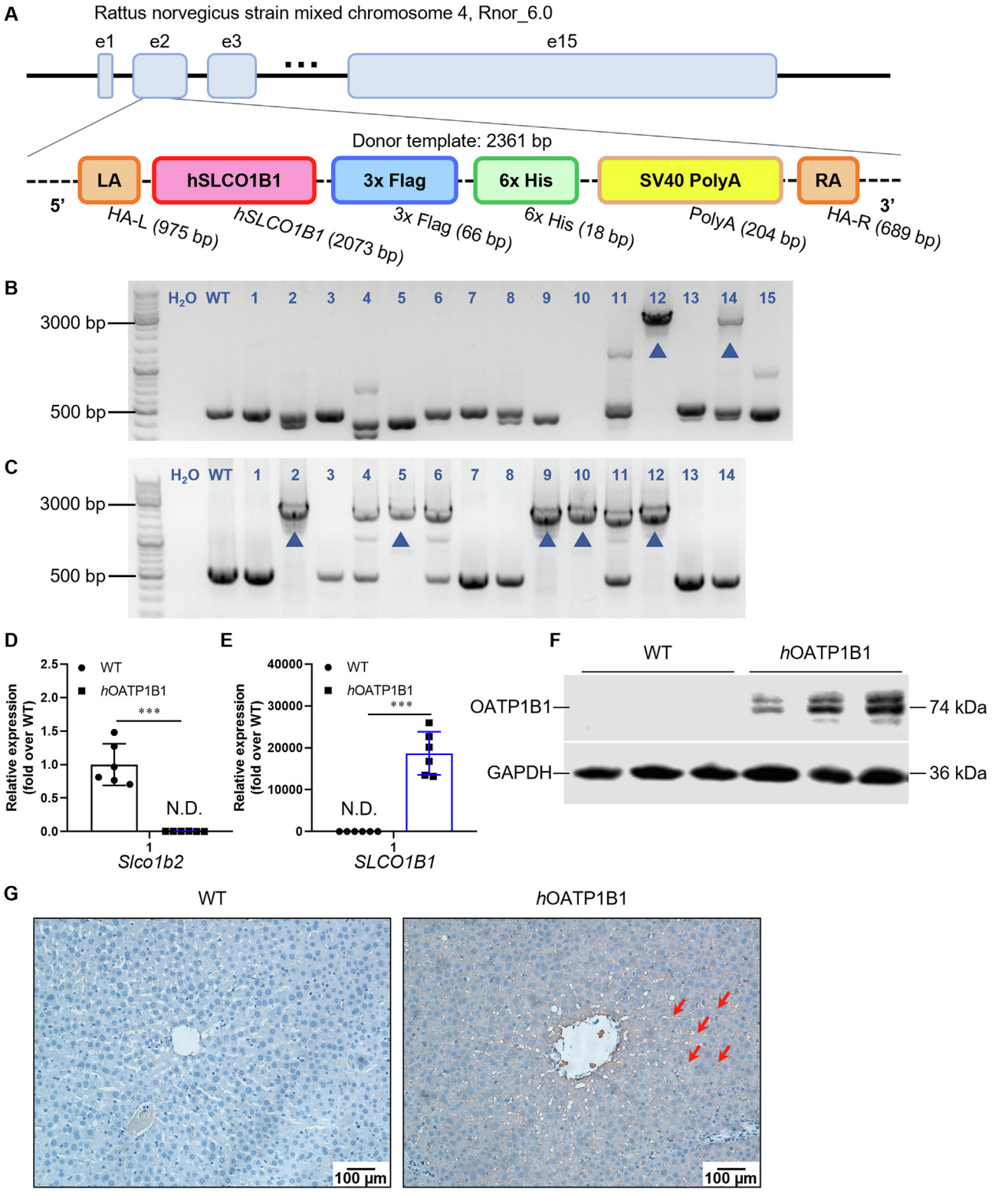

Figure 2 Generation of humanized OATP1B1 rats by CRISPR/Cas9. (A) The strategy for the generation of the *h*OATP1B1 rat model. The donor template (2361 bp) was inserted at the second exon. Mutations in the F0 generation (B) and F2 generation (C). H_2O, negative control; WT, blank control; Arrow, mutant band. The expression of *Slco1b2* (D) and *SLCO1B1* (E) in WT and *h*OATP1B1 rats. Data are shown as mean ± SD ($n = 6$). N.D., not detected. ***$P < 0.001$ compared with the WT group. (F) The protein expression of OATP1B1 in the liver (Western blot). (G) OATP1B1 is highly expressed on the sinusoidal membrane of the *h*OATP1B1 rat liver (shown in brown).

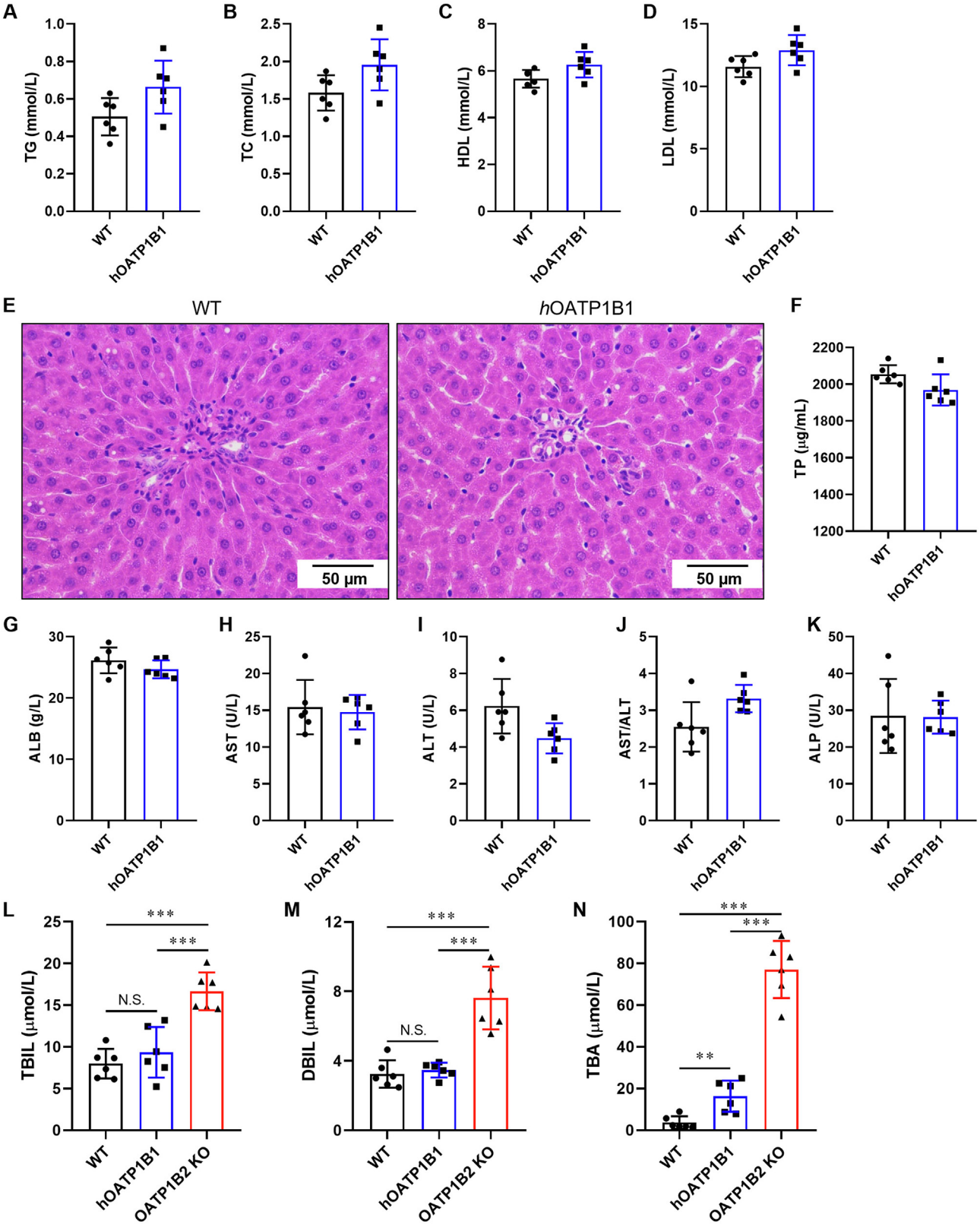

Figure 3 Physiological characterization of *h*OATP1B1 rats. (A)−(D) Blood lipids indexes in the serum of WT and *h*OATP1B1 rats, including TG, TC, HDL-C, and LDL-C. (E) H&E staining of liver tissue sections. Scale bars, 50 μm in length. (F)−(K) Indicators of liver function in the serum of WT and *h*OATP1B1 rats, including TP, ALB, AST, ALT, AST/ALT, and ALP. (L)−(N) The contents of TBIL, DBIL, and TBA in the serum of WT, *h*OATP1B1, and OATP1B2 KO rats, respectively. Values are shown as mean ± SD ($n = 6$). $^{**}P < 0.01$ and $^{***}P < 0.001$.

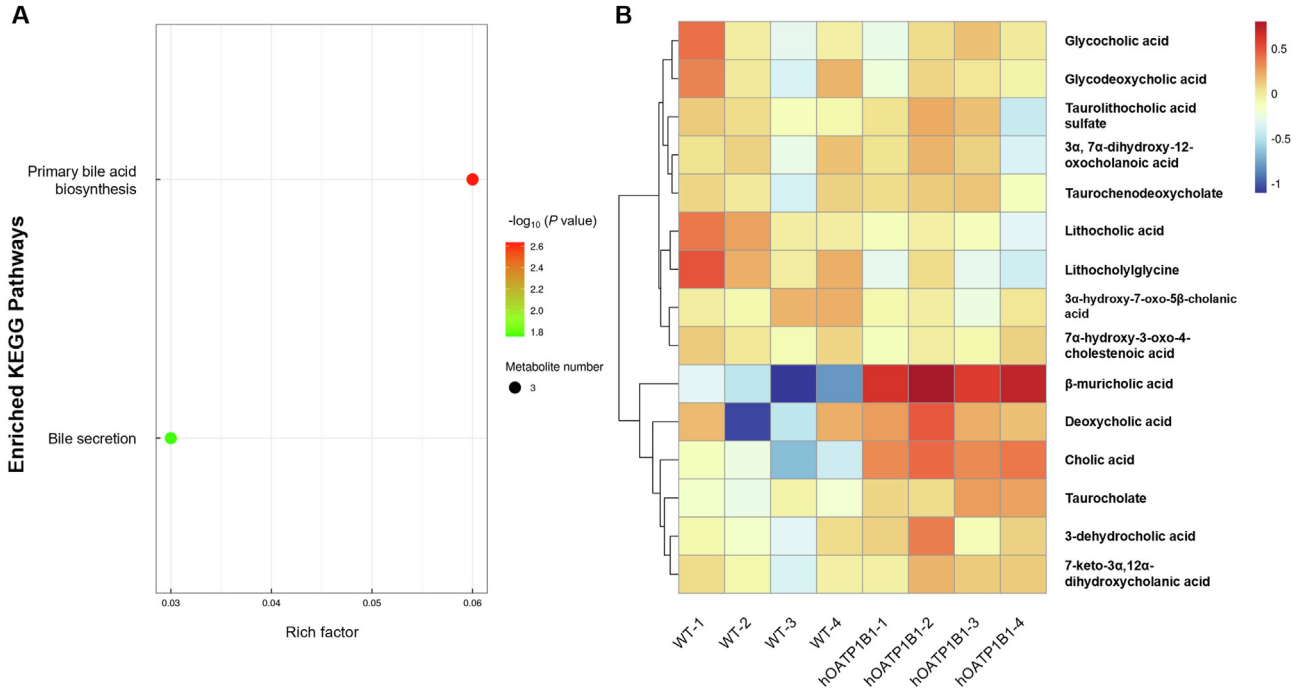

Figure 4 Effects of *SLCO1B1* gene insertion on bile acid-related pathway. (A) Differential abundance score and size of perturbed metabolic pathways between WT and *h*OATP1B1 rats. Size means the number of differential metabolites included in the pathway (KEGG database matched results). (B) Heat plot of the differential metabolites (bile acid pathway) between WT and *h*OATP1B1 rats ($n = 4$).

3.3. Pharmacokinetics of statins in WT, hOATP1B1, and OATP1B2 KO rats

The transport function of OATP1B1 is the key to evaluating the success of humanized rats. In this study, pitavastatin (5 mg/kg), rosuvastatin (10 mg/kg), and fluvastatin (5 mg/kg) were used to conduct pharmacokinetic experiments in WT, *h*OATP1B1, and OATP1B2 KO rats by oral gavage. The concentration−time curves and pharmacokinetic parameters are shown in Fig. 5A−C and Table 1, respectively. For pitavastatin, the pharmacokinetic behavior in *h*OATP1B1 rats was almost identical to that of WT rats, with no significant changes. However, compared to OATP1B2 KO rats, the $t_{1/2}$ and MRT_{0-t} were significantly shortened by 31.8% and 16.7%, the C_{max} and AUC_{0-t} were significantly decreased by 40.6% and 47.1%, and the V_d/F and CL/*F* were significantly increased by 33.9% and 94.7%, respectively. These results suggest that OATP1B1 plays the same role as OATP1B2 in the transport of pitavastatin. For rosuvastatin, the C_{max} and AUC_{0-t} of *h*OATP1B1 rats were 13.7% and 17.2% lower than those of OATP1B2 KO rats, while compared to WT rats, the C_{max} was significantly increased by 69.5%. These results indicated that, compared with OATP1B2, OATP1B1 was only partially involved in rosuvastatin transport. Unlike pitavastatin and rosuvastatin, the pharmacokinetic behavior of fluvastatin in *h*OATP1B1 rats was closer to that of OATP1B2 KO rats. Although the C_{max} of *h*OATP1B1 rats was decreased by 21.9% relative to OATP1B2 KO rats, the increase in C_{max} relative to WT rats was higher (66.4%). More importantly, the AUC_{0-t} in *h*OATP1B1 rats was not significantly different from OATP1B2 KO rats, but it was much higher than that in WT rats (an increase of 88%). These results showed that OATP1B1 was rarely involved in the transport of fluvastatin compared to OATP1B2. Based on the above pharmacokinetic results, OATP1B1 has different promoting effects on the uptake of different statins.

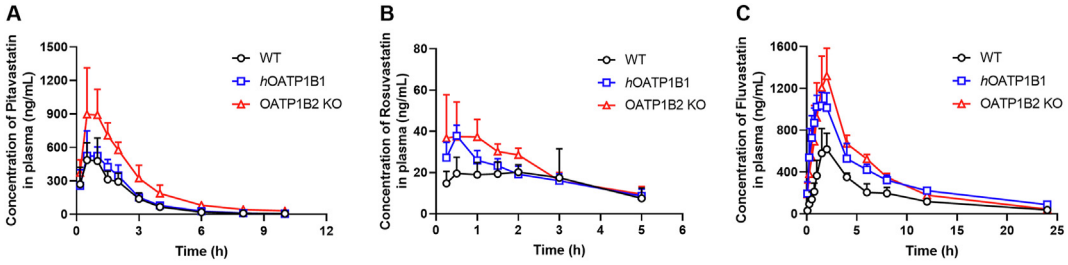

Figure 5 Pharmacokinetic profiles of statins in WT, *h*OATP1B1, and OATP1B2 KO rats. (A) Pitavastatin, 5 mg/kg. (B) Rosuvastatin, 10 mg/kg. (C) Fluvastatin, 5 mg/kg. All statins were administered intragastrically and the concentration of statins was quantified by LC−MS/MS. The concentration corresponding to each time point on the curve was presented as mean ± SD ($n = 6$).

Table 1 Pharmacokinetic parameters of pitavastatin, rosuvastatin, and fluvastatin in WT, *h*OATP1B1, and OATP1B2 KO rats.

PK parameter	Pitavastatin (5 mg/kg)			Rosuvastatin (10 mg/kg)			Fluvastatin (5 mg/kg)		
	WT	*h*OATP1B1	OATP1B2 KO	WT	*h*OATP1B1	OATP1B2 KO	WT	*h*OATP1B1	OATP1B2 KO
$t_{1/2}$ (h)	2.1 ± 0.7	1.5 ± 0.3$^{\#}$	2.2 ± 0.5	2.4 ± 1.6	2.5 ± 0.9	1.9 ± 0.6	7.1 ± 1.2	8.8 ± 1.0	5.3 ± 0.8
T_{max} (h)	0.8 ± 0.3	0.9 ± 0.4	0.8 ± 0.4	1.4 ± 0.9	0.5 ± 0.0	1.1 ± 0.9	1.8 ± 0.3	1.5 ± 0.5	1.9 ± 0.2
C_{max} (ng/mL)	583.3 ± 147.0	594.1 ± 187.3$^{\#}$	999.9 ± 309.1	22.3 ± 6.6	37.8 ± 5.2**	43.8 ± 12.1	642.7 ± 174.8	1069.3 ± 117.4$^{***\#\#}$	1369.3 ± 179.0
AUC_{0-t} (h·ng/mL)	1176.0 ± 213.4	1369.1 ± 181.1$^{\#\#\#}$	2586.8 ± 476.2	72.7 ± 18.9	92.6 ± 16.6	111.9 ± 18.6	4191.7 ± 198.2	7879.3 ± 842.9***	8161.1 ± 667.8
V_d/F (L/kg)	12.9 ± 5.7	7.9 ± 1.8$^{\#}$	5.9 ± 1.0	311.7 ± 57.5	280.3 ± 50.8$^{\#}$	196.8 ± 31.6	11.2 ± 1.8	7.1 ± 1.2$^{***\#\#\#}$	4.5 ± 0.6
CL/F (L/h/kg)	4.3 ± 0.8	3.7 ± 0.5$^{\#\#\#}$	1.9 ± 0.4	114.8 ± 54.2	85.7 ± 32.3	74.5 ± 18.6	1090.2 ± 43.0	559.3 ± 53.4***	590.9 ± 54.9
MRT_{0-t} (h)	1.9 ± 0.3	2.0 ± 0.2$^{\#}$	2.4 ± 0.3	2.1 ± 0.2	2.0 ± 0.1	1.9 ± 0.3	6.9 ± 0.8	7.0 ± 0.3$^{\#\#}$	6.0 ± 0.6

The data are shown as mean ± SD (n = 6), and the pharmacokinetic parameters were calculated with non-compartmental analysis. A two-tailed Student t-test was used for statistical analysis. $^{**}P < 0.01$ and $^{***}P < 0.001$ compared to WT rats; $^{\#}P < 0.05$, $^{\#\#}P < 0.01$, and $^{\#\#\#}P < 0.001$ compared to OATP1B2 KO rats.

3.4. Validation of statins uptake by OATP1B1 overexpressed cells

To further validate the contribution of OATP1B1 and OATP1B2 in statins transport, we constructed OATP1B1 and OATP1B2 overexpressed cells *in vitro*. The pCDH plasmid was used as a blank control. As shown in Fig. 6A, after transfection of HEK293T cells for 24 h, the green fluorescence was observed, indicating that the transporters were successfully expressed. The Western blot results also showed that OATP1B1 was highly expressed in HEK293T cells (Fig. 6B). After incubation with statins (10 μmol/L) for 1 h, the concentrations of pitavastatin, rosuvastatin, and fluvastatin were detected, as shown in Fig. 6C−E. The concentration of pitavastatin in OATP1B1 overexpressed cells was much higher than that in pCDH cells, while there was no significant difference in pitavastatin concentration between OATP1B1 and OATP1B2 cells. This data revealed that OATP1B1 and OATP1B2 had the same transport capacity for pitavastatin. The transport results of rosuvastatin and fluvastatin were similar. The concentrations of rosuvastatin and fluvastatin in OATP1B1 overexpressed cells were significantly higher than those in pCDH cells, but significantly lower than those in OATP1B2 overexpressed cells. This suggests that OATP1B1 has less transport effect on rosuvastatin and fluvastatin than OATP1B2.

3.5. Molecular docking of statins with OATP1B1

Our data suggest that OATP1B1 contributes differently to the uptake of pitavastatin, rosuvastatin, and fluvastatin. Docking simulations were performed to investigate the interaction mechanism between statins and OATP1B1. The results showed that different statins exhibited favorable docking with the transport cavity of OATP1B1, with low predicted binding affinities of −6.594 kcal/mol for pitavastatin, −6.582 kcal/mol for rosuvastatin, and −6.227 kcal/mol for fluvastatin in the extracellular domains (Fig. 7A), respectively. In addition, the binding energy in the cavity of transmembrane helices (Fig. 7B) was −7.071 kcal/mol for pitavastatin, −6.997 kcal/mol for rosuvastatin, and −6.908 kcal/mol for fluvastatin, respectively. These results fit well with the different binding affinities of these statins to OATP1B1.

4. Discussion

Statins have shown excellent efficacy in cardiovascular disease treatment by reducing LDL-C, while their use is restricted to occasional adverse events (AEs), mainly SAMS[31]. The occurrence of AEs can worsen the patients' compliance with statins, which is not conducive to clinical benefits. Statin therapy should be personalized, considering the individual patient characteristics and drug-specific factors (such as metabolism and transport properties) that may lead to AEs[32]. Although the use of high-intensity statins (atorvastatin or rosuvastatin) is recommended, it is important to recognize that the use of less-intensity statins may be needed to reduce the risk of AEs and optimize adherence. Therefore, studying the characteristics of statins with different intensities is of great value for their safe use. In this study, the contribution of OATP1B1 to rosuvastatin (high intensity), pitavastatin (moderate intensity), and fluvastatin (low intensity) was investigated in humanized rats.

Liver-humanized animals have become invaluable tools for simulating the physiological and pathological characteristics of

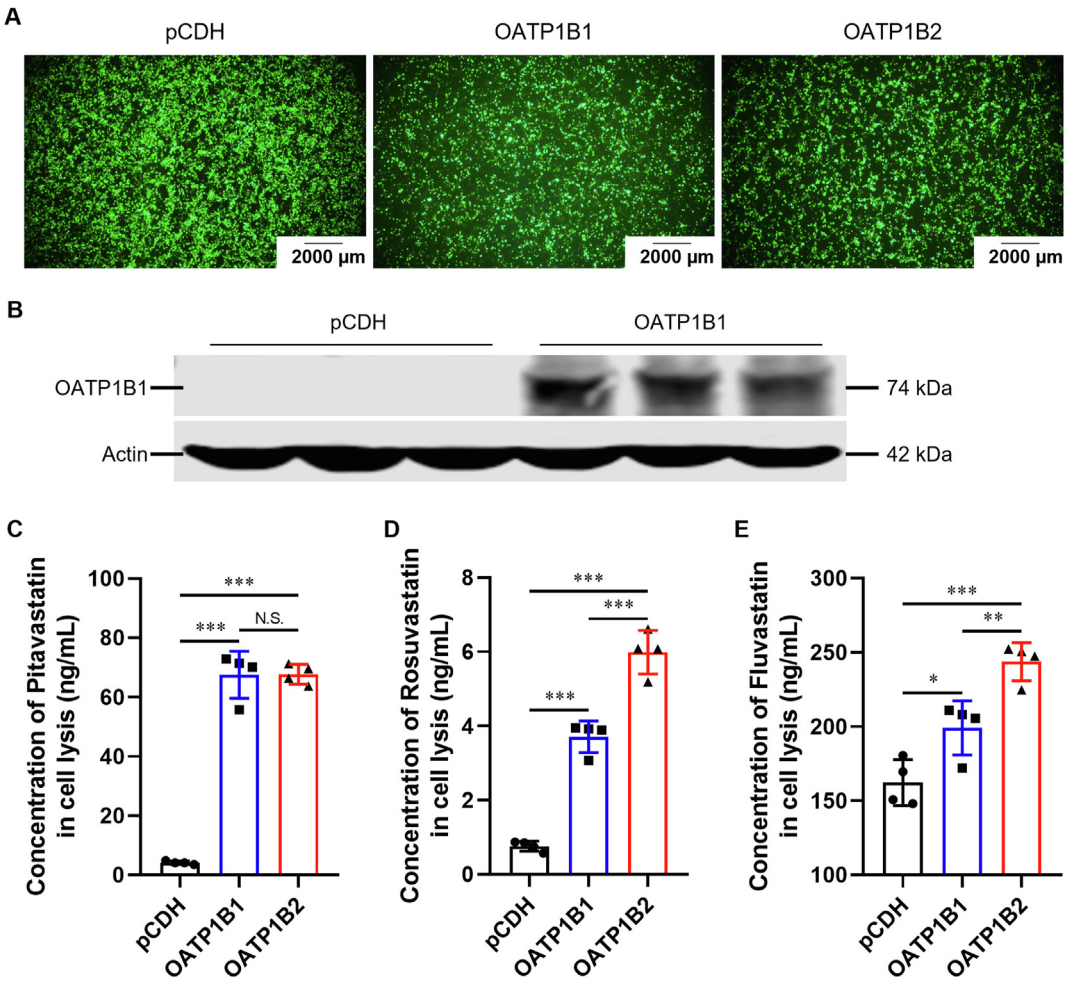

Figure 6 Transport of statins in OATP1B1 overexpression cells. (A) Green fluorescence after transfection of HEK293T cells for 24 h. Scale bars, 2000 μm. (B) Protein expression of OATP1B1 (Western blot). The concentration of pitavastatin (C), rosuvastatin (D), and fluvastatin (E) in cell lysis. Data are shown as mean ± SD ($n = 4$). *$P < 0.05$, **$P < 0.01$, and ***$P < 0.001$.

the human liver, and can also be used for various biomedical applications[24,25,33]. Humanized OATP1B1 mice have been generated and characterized, and considerable research has been conducted on the function of human OATP1B1, including a series of studies on transporter uptake of different drugs[34–36]. However, for the *SLCO1B1* transgenic liver, immunohistochemical staining was strongest only around the portal vein, which is inconsistent with its expression location in the human liver. Even more regrettably, no functional activity was found when the pharmacokinetics of pitavastatin and rosuvastatin were studied[23]. CRISPR/Cas9 technology plays a key role in the construction of humanized animal models and promotes the generation of *h*OATP1B1 rats. In contrast, the *h*OATP1B1 rats we characterized are more similar in expression and function to the real situation in humans. In addition, compared with mice, the physiological and pathological characteristics of rats are also similar to those of humans, and are widely used in human disease research[37]. Moreover, rats are considered the first choice for *in vivo* pharmacokinetics (including drug metabolism and transport) and drug−drug interaction studies[37,38].

OATP1B1 is crucial for hepatic uptake of numerous endogenous compounds and a broad range of drug substrates[18]. Bilirubin and bile acids are the most representative endogenous substrates of OATP1B1. The absence of OATP1B2 in rats or functional impairment of human OATP1B1 can significantly increase serum bilirubin levels and then induce the occurrence of hyperbilirubinemia[26,39]. However, in the serum of *h*OATP1B1 rats, there was no significant difference in the concentration of both TBIL and DBIL compared to WT rats. Although the TBA content of *h*OATP1B1 rats was higher than that of WT rats, it was significantly lower than that of OATP1B2 KO rats. These results suggest that *h*OATP1B1 rats have the function of transporting endogenous substrates and can also serve as a novel model of hyperbilirubinemia disease.

In vitro studies have shown that OATP1B1 and OATP1B3 contribute differently to the absorption of different statins in hepatic uptake. Both OATP1B1 and OATP1B3 are expressed on the basolateral membrane of the liver, but their specific distribution is different[40]. OATP1B1 is expressed throughout the hepatic lobule, while OATP1B3 is mainly expressed around the central vein. This resulted in a much higher expression level of OATP1B1 than OATP1B3[40,41]. In addition, recent studies have shown that the role of OATP1B3 is more complex than previously understood, and OATP1B1 is more likely to be the true ortholog of rodent OATP1B2[20,42,43]. By comparing the pharmacokinetic characteristics of statins in WT, *h*OATP1B1, and OATP1B2 KO rats, we

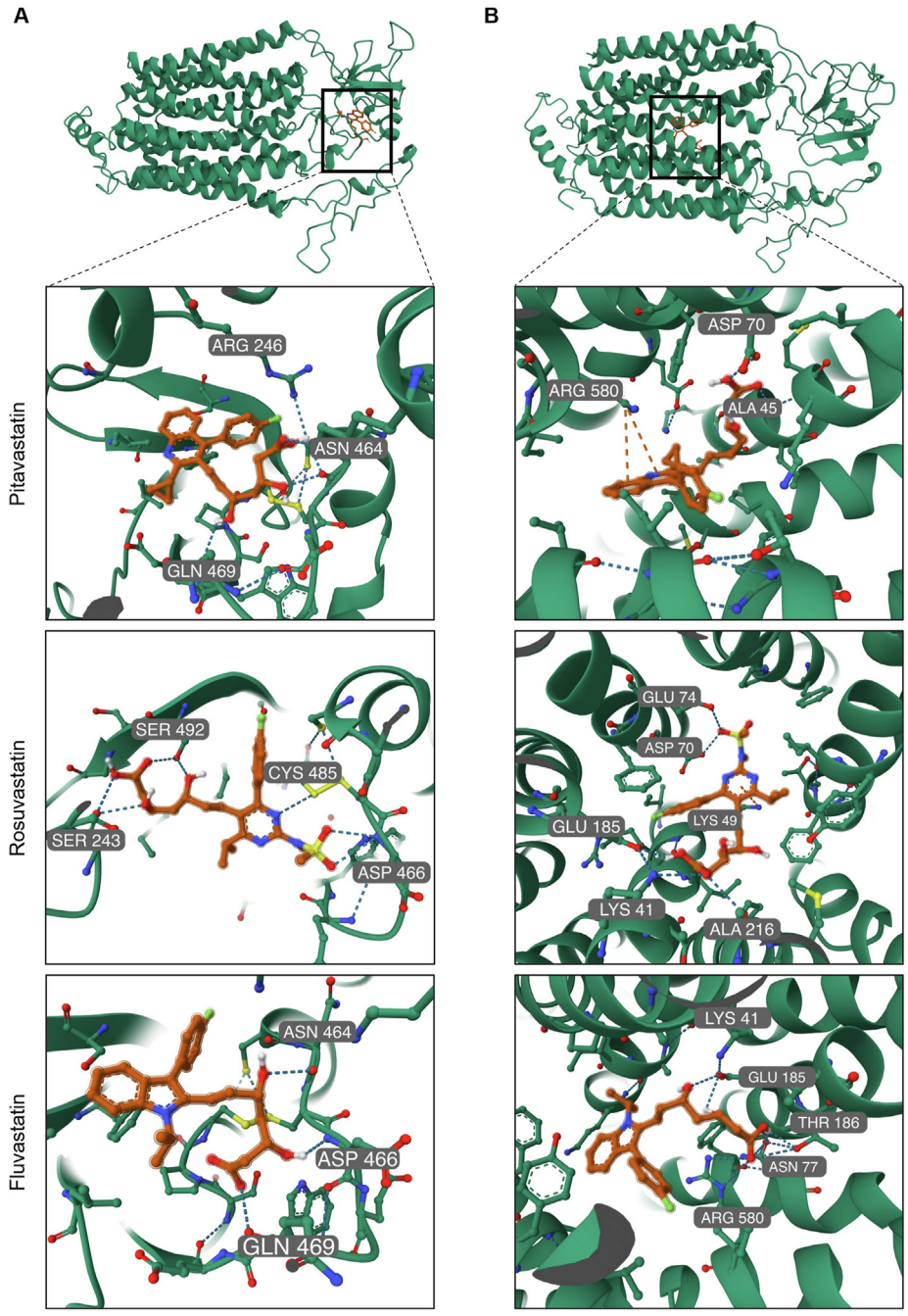

Figure 7 The binding modes and enzyme−substrate interactions of pitavastatin, rosuvastatin, and fluvastatin with OATP1B1 in the cavity of extracellular domains (A) and transmembrane helices (B).

first verified the contribution of OATP1B1 to the overall uptake of pitavastatin, rosuvastatin, and fluvastatin in rodents. Our results showed that OATP1B1 was involved in the exposure levels of most pitavastatin (86.3%), some rosuvastatin (49.2%), and a small amount of fluvastatin (7.1%) in the body (Supporting Information Table S4). Excitingly, the results we obtained are consistent with those previously reported[2,44,45]. In addition, molecular docking analysis further confirmed the binding affinities of statins with OATP1B1. It is worth noting that the contribution of OATP1B1 to the uptake of fluvastatin is controversial[2,14,46]. Most of the conclusions on OATP1B1 involved in partial uptake of fluvastatin came from *in vitro* results (our *in vitro* results also reached the same conclusion, Supporting Information Table S5). From another perspective, the conclusions (seldom contribution) we drew from *in vivo* experiments in *h*OATP1B1 rats are closer to the AHA Scientific Statement[2].

The guidelines developed by the U.S. Food and Drug Administration (FDA) are important references for evaluating drug absorption and metabolism. According to the FDA decision tree, if the compound has active hepatocyte uptake, the uptake of OATP1B1-overexpressed cell lines should be investigated, and the *in vivo* drug interaction study with a single-dose rifampin or

cyclosporin as perpetrator should be conducted to confirm that the investigational drug is an OATP1B1 substrate[47]. The emergence of *h*OATP1B1 rats will make the evaluation method more direct and convenient. As mentioned above, numerous *in vitro* and clinical studies have evaluated the impact of *SLCO1B1* SNPs (especially *SLCO1B1* 388 A > G and 521 T > C) on interindividual differences in drug disposition and response[18]. Based on *h*OATP1B1 rats, site-specific base mutations in the CDS region can be performed to construct an *SLCO1B1* SNP rat model, which will help to identify the importance of OATP1B1.

5. Conclusions

This study characterized a novel humanized *SLCO1B1* transgenic rat model and evaluated the contribution of human OATP1B1 to statin uptake. The *h*OATP1B1 rat will be a promising animal model for improving the prediction of human drug transport.

Acknowledgments

This work was supported by grants from the National Natural Science Foundation of China (82274010), the Science and Technology Commission of Shanghai Municipality (18430760400, China), the East China Normal University (ECNU) Medicine and Health Joint Fund (2022JKXYD09004, China), the Jointed PI Program from Shanghai Changning Maternity and Infant Health Hospital, and ECNU Construction Fund of Innovation and Entrepreneurship Laboratory. Also, this work was supported from ECNU multifunctional Platform for Innovation (011) and the Instruments Sharing Platform of School of Life Sciences, East China Normal University (Shanghai, China).

Author contributions

Xin Wang was responsible for the conception and design of the study. Yuanjin Zhang and Xin Wang designed the experiments. Yuanjin Zhang, Junze Huang, Shengbo Huang, Jie Liu, and Luyao Deng performed the experiments. Yuanjin Zhang, Junze Huang, Yuanqing Guo, and Xin Wang analyzed the data. Yuanjin Zhang and Chenmeizi Liang drafted the manuscript. Bingyi Yao and Xin Wang supervised the study and revised the manuscript. All authors critically reviewed and approved the final version of the manuscript.

Conflicts of interest

The authors declare no conflicts of interest.

Appendix A. Supporting information

Supporting data to this article can be found online at https://doi.org/10.1016/j.apsb.2023.12.019.

References

1. Guan ZW, Wu KR, Li R, Yin Y, Li XL, Zhang SF, et al. Pharmacogenetics of statins treatment: efficacy and safety. *J Clin Pharm Thera* 2019;**44**:858–67.
2. Newman CB, Preiss D, Tobert JA, Jacobson TA, Page 2nd RL, Goldstein LB, et al. Statin safety and associated adverse events: a scientific statement from the American Heart Association. *Arterioscler Thromb Vasc Biol* 2019;**39**:e38–81.
3. Sultan S, Khan SU, Holden K, Hendi AA, Saeed S, Abbas A, et al. Reducing the threshold of primary prevention of cardiovascular disease to 10% over 10 years: the implications of altered intensity "statin" therapy guidance. *Curr Probl Cardiol* 2023;**48**:101486.
4. Dolivo DM, Reed CR, Gargiulo KA, Rodrigues AE, Galiano RD, Mustoe TA, et al. Anti-fibrotic effects of statin drugs: a review of evidence and mechanisms. *Biochem Pharmacol* 2023;**214**:115644.
5. Hassan W, Yekta BG, Nabavi SM, Banach M, Rezabakhsh A. The progress and research trends of statin medications: advanced epidemiological and bibliometrical assessment. *Curr Probl Cardiol* 2023;**48**:101638.
6. Rabar S, Harker M, O'Flynn N, Wierzbicki AS, Guideline Development G. Lipid modification and cardiovascular risk assessment for the primary and secondary prevention of cardiovascular disease: summary of updated NICE guidance. *BMJ* 2014;**349**:g4356.
7. Uspst Force, Mangione CM, Barry MJ, Nicholson WK, Cabana M, Chelmow D, et al. Statin use for the primary prevention of cardiovascular disease in adults: US preventive services task force recommendation statement. *JAMA* 2022;**328**:746–53.
8. Vell MS, Loomba R, Krishnan A, Wangensteen KJ, Trebicka J, Creasy KT, et al. Association of statin use with risk of liver disease, hepatocellular carcinoma, and liver-related mortality. *JAMA Netw Open* 2023;**6**:e2320222.
9. Liu C, Shen M, Tan WLW, Chen IY, Liu Y, Yu X, et al. Statins improve endothelial function *via* suppression of epigenetic-driven EndMT. *Nat Cardiovasc Res* 2023;**2**:467–85.
10. Dicken W, Mehta A, Karagiannis A, Jain V, Vavuranakis M, Sperling L, et al. Statin associated muscle symptoms: an update and review. *Prog Cardiovasc Dis* 2022;**75**:40–8.
11. Lamprecht Jr DG, Saseen JJ, Shaw PB. Clinical conundrums involving statin drug–drug interactions. *Prog Cardiovasc Dis* 2022;**75**:83–9.
12. Wiggins BS, Saseen JJ, Page 2nd RL, Reed BN, Sneed K, Kostis JB, et al. Recommendations for management of clinically significant drug-drug interactions with statins and select agents used in patients with cardiovascular disease: a scientific statement from the American Heart Association. *Circulation* 2016;**134**:e468–95.
13. Konig J, Seithel A, Gradhand U, Fromm MF. Pharmacogenomics of human OATP transporters. *Naunyn-Schmiedeberg's Arch Pharmacol* 2006;**372**:432–43.
14. Kalliokoski A, Niemi M. Impact of OATP transporters on pharmacokinetics. *Br J Pharmacol* 2009;**158**:693–705.
15. Shitara Y, Maeda K, Ikejiri K, Yoshida K, Horie T, Sugiyama Y. Clinical significance of organic anion transporting polypeptides (OATPs) in drug disposition: their roles in hepatic clearance and intestinal absorption. *Biopharm Drug Dispos* 2013;**34**:45–78.
16. Kellick K. Organic ion transporters and statin drug interactions. *Curr Atherosclerosis Rep* 2017;**19**:65.
17. Konig J, Cui Y, Nies AT, Keppler D. A novel human organic anion transporting polypeptide localized to the basolateral hepatocyte membrane. *Am J Physiol Gastrointest Liver Physiol* 2000;**278**:G156–64.
18. Lee HH, Ho RH. Interindividual and interethnic variability in drug disposition: polymorphisms in organic anion transporting polypeptide 1B1 (OATP1B1; SLCO1B1). *Br J Clin Pharmacol* 2017;**83**:1176–84.
19. Tirona RG, Leake BF, Merino G, Kim RB. Polymorphisms in OATP-C: identification of multiple allelic variants associated with altered transport activity among European- and African-Americans. *J Biol Chem* 2001;**276**:35669–75.
20. Choudhuri S, Klaassen CD. Elucidation of OATP1B1 and 1B3 transporter function using transgenic rodent models and commonly known single nucleotide polymorphisms. *Toxicol Appl Pharmacol* 2020;**399**:115039.
21. Roth M, Obaidat A, Hagenbuch B. OATPs, OATs and OCTs: the organic anion and cation transporters of the *SLCO* and *SLC22A* gene superfamilies. *Br J Pharmacol* 2012;**165**:1260–87.

22. Chu X, Bleasby K, Evers R. Species differences in drug transporters and implications for translating preclinical findings to humans. *Expet Opin Drug Metabol Toxicol* 2013;**9**:237−52.
23. Salphati L, Chu X, Chen L, Prasad B, Dallas S, Evers R, et al. Evaluation of organic anion transporting polypeptide 1B1 and 1B3 humanized mice as a translational model to study the pharmacokinetics of statins. *Drug Metab Dispos* 2014;**42**:1301−13.
24. Kazuki Y, Kobayashi K, Hirabayashi M, Abe S, Kajitani N, Kazuki K, et al. Humanized UGT2 and CYP3A transchromosomic rats for improved prediction of human drug metabolism. *Proc Natl Acad Sci U S A* 2019;**116**:3072−81.
25. Devoy A, Bunton-Stasyshyn RK, Tybulewicz VL, Smith AJ, Fisher EM. Genomically humanized mice: technologies and promises. *Nat Rev Genet* 2011;**13**:14−20.
26. Ma X, Shang X, Qin X, Lu J, Liu M, Wang X. Characterization of organic anion transporting polypeptide 1b2 knockout rats generated by CRISPR/Cas9: a novel model for drug transport and hyperbilirubinemia disease. *Acta Pharm Sin B* 2020;**10**:850−60.
27. Sun D, Lu J, Zhang Y, Liu J, Liu Z, Yao B, et al. Characterization of a novel CYP1A2 knockout rat model constructed by CRISPR/Cas9. *Drug Metab Dispos* 2021;**49**:638−47.
28. Shang M, Yang H, Yang R, Chen T, Fu Y, Li Y, et al. The folate cycle enzyme MTHFD2 induces cancer immune evasion through PD-L1 up-regulation. *Nat Commun* 2021;**12**:1940.
29. Ma X, Qin X, Shang X, Liu M, Wang X. Organic anion transport polypeptide 1b2 selectively affects the pharmacokinetic interaction between paclitaxel and sorafenib in rats. *Biochem Pharmacol* 2019;**169**:113612.
30. Eberhardt J, Santos-Martins D, Tillack AF, Forli S. AutoDock vina 1.2.0: new docking methods, expanded force field, and python bindings. *J Chem Inf Model* 2021;**61**:3891−8.
31. Cohen JD, Brinton EA, Ito MK, Jacobson TA. Understanding statin use in America and Gaps in Patient Education (USAGE): an internet-based survey of 10,138 current and former statin users. *J Clin Lipidol* 2012;**6**:208−15.
32. Wiggins BS, Backes JM, Hilleman D. Statin-associated muscle symptoms—a review: individualizing the approach to optimize care. *Pharmacotherapy* 2022;**42**:428−38.
33. Zhang L, Ge JY, Zheng YW, Sun Z, Wang C, Peng Z, et al. Survival-assured liver injury preconditioning (SALIC) enables robust expansion of human hepatocytes in Fah$^{-/-}$ Rag2$^{-/-}$ IL2rg$^{-/-}$ rats. *Adv Sci* 2021;**8**:e2101188.
34. van de Steeg E, van der Kruijssen CM, Wagenaar E, Burggraaff JE, Mesman E, Kenworthy KE, et al. Methotrexate pharmacokinetics in transgenic mice with liver-specific expression of human organic anion-transporting polypeptide 1B1 (SLCO1B1). *Drug Metab Dispos* 2009;**37**:277−81.
35. Higgins JW, Bao JQ, Ke AB, Manro JR, Fallon JK, Smith PC, et al. Utility of *Oatp1a/1b*-knockout and *OATP1B1/3*-humanized mice in the study of OATP-mediated pharmacokinetics and tissue distribution: case studies with pravastatin, atorvastatin, simvastatin, and carboxydichlorofluorescein. *Drug Metab Dispos* 2014;**42**:182−92.
36. van de Steeg E, van Esch A, Wagenaar E, Kenworthy KE, Schinkel AH. Influence of human OATP1B1, OATP1B3, and OATP1A2 on the pharmacokinetics of methotrexate and paclitaxel in humanized transgenic mice. *Clin Cancer Res* 2013;**19**:821−32.
37. Lu J, Shang X, Yao B, Sun D, Liu J, Zhang Y, et al. The role of CYP1A1/2 in cholesterol ester accumulation provides a new perspective for the treatment of hypercholesterolemia. *Acta Pharm Sin B* 2023;**13**:648−61.
38. Lu J, Liu J, Guo Y, Zhang Y, Xu Y, Wang X. CRISPR-Cas9: a method for establishing rat models of drug metabolism and pharmacokinetics. *Acta Pharm Sin B* 2021;**11**:2973−82.
39. van de Steeg E, Stranecky V, Hartmannova H, Noskova L, Hrebicek M, Wagenaar E, et al. Complete OATP1B1 and OATP1B3 deficiency causes human Rotor syndrome by interrupting conjugated bilirubin reuptake into the liver. *J Clin Invest* 2012;**122**:519−28.
40. Konig J, Cui Y, Nies AT, Keppler D. Localization and genomic organization of a new hepatocellular organic anion transporting polypeptide. *J Biol Chem* 2000;**275**:23161−8.
41. Briz O, Romero MR, Martinez-Becerra P, Macias RI, Perez MJ, Jimenez F, et al. OATP8/1B3-mediated cotransport of bile acids and glutathione: an export pathway for organic anions from hepatocytes?. *J Biol Chem* 2006;**281**:30326−35.
42. Malagnino V, Duthaler U, Seibert I, Krahenbuhl S, Meyer Zu Schwabedissen HE. OATP1B3−1B7 (LST-3TM12) is a drug transporter that affects endoplasmic reticulum access and the metabolism of ezetimibe. *Mol Pharmacol* 2019;**96**:128−37.
43. Malagnino V, Hussner J, Issa A, Midzic A, Meyer Zu Schwabedissen HE. OATP1B3−1B7, a novel organic anion transporting polypeptide, is modulated by FXR ligands and transports bile acids. *Am J Physiol Gastrointest Liver Physiol* 2019;**317**:G751−62.
44. Hirano M, Maeda K, Shitara Y, Sugiyama Y. Contribution of OATP2 (OATP1B1) and OATP8 (OATP1B3) to the hepatic uptake of pitavastatin in humans. *J Pharmacol Exp Therapeut* 2004;**311**:139−46.
45. Kitamura S, Maeda K, Wang Y, Sugiyama Y. Involvement of multiple transporters in the hepatobiliary transport of rosuvastatin. *Drug Metab Dispos* 2008;**36**:2014−23.
46. Kellick KA, Bottorff M, Toth PP. The National Lipid Association's Safety Task F. A clinician's guide to statin drug−drug interactions. *J Clin Lipidol* 2014;**8**:S30−46.
47. International Transporter Consortium, Giacomini KM, Huang SM, Tweedie DJ, Benet LZ, Brouwer KL, et al. Membrane transporters in drug development. *Nat Rev Drug Discov* 2010;**9**:215−36.